

Influence of Zr dopant on the dielectric properties and Curie temperatures of $\text{Ba}(\text{Zr}_x\text{Ti}_{1-x})\text{O}_3$ ($0 \leq x \leq 0.12$) ceramics

S.J. Kuang, X.G. Tang,* L.Y. Li, Y.P. Jiang and Q.X. Liu

School of Physics and Optoelectric Engineering, Guangdong University of Technology, Guangzhou Higher Education Mega Center, Guangzhou 510006, PR China

Received 26 January 2009; revised 5 March 2009; accepted 5 March 2009

Available online 14 March 2009

$\text{Ba}(\text{Zr}_x\text{Ti}_{1-x})\text{O}_3$ (BZT, $0 \leq x \leq 0.12$, step = 0.02) ceramics have been prepared by the solid solution reaction method. The Curie temperature decreased nonlinearly from 131 to 74 °C with increases x from 0 to 0.12 in BZT ceramics. While the diffusion factor increase from 1.06 to 1.64 with increases x from 0 to 0.12, implying a composition-induced diffuse transition. The phase transition temperature of tetragonal to orthorhombic structure (T_{o-t}) increases with increasing of Zr content, forming a pinched phase transition.

© 2009 Acta Materialia Inc. Published by Elsevier Ltd. All rights reserved.

Keywords: Electroceramics; Perovskites; Dielectric properties; Phase transformations; Diffusion

Perovskite-type titanate oxides ATiO_3 (where A stands for alkaline-earth ions such as Pb, Ca, Sr and Ba) have attracted much attention in the past decades because they are very important ferroelectric, dielectric and pyroelectric materials with wide applications in capacitor, piezoelectric, pyroelectric, memory storage and microwave devices [1–5]. One of the members of the ATiO_3 series, BaTiO_3 (BT), is the most widely studied ferroelectric material and is known to have excellent properties, such as a large electromechanical coupling factor, high permittivity with abrupt change near the Curie temperature and low loss tangent. Isovalent cation substitution for host ones in perovskite lattice—e.g. Zr^{4+} , Sn^{4+} for Ti^{4+} and Sr^{2+} , Ca^{2+} for Ba^{2+} —plays a very important role in these modification mechanisms [6]. Zr^{4+} has been chosen to form $\text{Ba}(\text{Zr}_x\text{Ti}_{1-x})\text{O}_3$, which is the important composition for dielectric in multilayer ceramics capacitors [7]. Like PbTiO_3 and PbZrO_3 , the BaTiO_3 and BaZrO_3 materials can also form the $\text{Ba}(\text{Zr}_x\text{Ti}_{1-x})\text{O}_3$ solid solution, and furthermore, Zr^{4+} is chemically more stable than Ti^{4+} [8]. Zr^{4+} -substituted BaTiO_3 ceramics show several interesting features in dielectric behavior. The phase transition of this material can change from a normal ferroelectric behavior to relaxor ferroelectric behavior. For Zr contents $x > 8$ at.%, the $\text{Ba}(\text{Zr}_x\text{Ti}_{1-x})\text{O}_3$

ceramics show a broad dielectric permittivity–temperature curve near T_m . When the Zr content is less than 10 at.%, the material shows normal ferroelectric behavior. As the Zr content increases, the phase transition temperatures approach each other, resulting in a pinched phase transition. When the Zr content reaches about 20 at.%, only one phase transition exists. And at around 27 at.% Zr-doping, $\text{Ba}(\text{Zr}_x\text{Ti}_{1-x})\text{O}_3$ ceramics show typical diffuse paraelectric-to-ferroelectric phase transition behavior, with further increasing Zr content, and typical relaxor behavior can be detected [9]. In addition, the electrical property of ATiO_3 perovskite ferroelectric ceramics can be controlled by minor modification of the dopants without serious affecting other properties [10]. A few reports in the literature have noted the effect of Zr content on the phase transition temperature of BaTiO_3 ceramics [11], such as cubic paraelectric to tetragonal ferroelectric (T_c) and the tetragonal ferroelectric to orthorhombic ferroelectric transition temperature (T_{o-t}).

In this work, the $\text{Ba}(\text{Zr}_x\text{Ti}_{1-x})\text{O}_3$ ($0 \leq x \leq 0.12$) ceramics were prepared by the solid state reaction method. The effects of Zr doping on the dielectric, Curie temperature, phase transition characteristics and diffusivity have been studied.

$\text{Ba}(\text{Zr}_x\text{Ti}_{1-x})\text{O}_3$ (with composition $x = 0, 0.02, 0.04, 0.06, 0.08, 0.10, 0.12$; hereafter abbreviated as BT, BZT2, BZT4, BZT6, BZT8, BZT10 and BZT12, respectively) ceramics were synthesized by the conventional mixed-oxide method. High-purity (99.0%) barium

* Corresponding author. Fax: +86 20 3932 2265; e-mail: xgtang6@yahoo.com

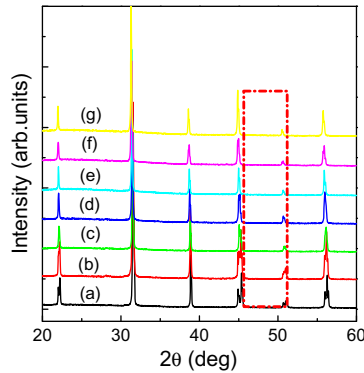


Figure 1. XRD patterns of $\text{Ba}(\text{Zr}_x\text{Ti}_{1-x})\text{O}_3$ ceramics with various x : (a) 0, (b) 0.02, (c) 0.04, (d) 0.06, (e) 0.08, (f) 0.10 and (g) 0.12.

carbonate (BaCO_3), zirconium dioxide (ZrO_2) and titanium dioxide (TiO_2) powders were used as starting raw materials. The powders were weighed according to the composite formula $\text{Ba}(\text{Zr}_x\text{Ti}_{1-x})\text{O}_3$ and ball-milled for 24 h in ethanol. After drying, the mixtures were calcined at 1100°C for 4 h in a high-purity alumina crucible, then ball-milled and dried again. The resulting powders were mixed thoroughly with the PVA binder solution and after granulation, disk pellets were prepared at 20 MPa pressure. PVA was burned out in the electric furnace at 650°C . The disk samples were finally sintered at 1400°C for 4 h in air. For the measurement of electrical properties, both sides of the samples were polished, silver paste was applied, followed by firing at 650°C for 30 min to form the electrodes.

The crystal structures of ceramic samples were characterized by X-ray diffraction (XRD; Philips Expert system, $\text{Cu K}\alpha$). The temperature dependence of relative permittivity ϵ_r and loss tangent of the samples was measured using a programmable furnace with impedance analyzer (HP 4192A Impedance Analyzer) at different frequencies from 1 to 100 kHz in a temperature range of 25 – 250°C .

Figure 1 shows the XRD patterns of $\text{Ba}(\text{Zr}_x\text{Ti}_{1-x})\text{O}_3$ ceramics with various x values from 0 to 0.12. The XRD analysis revealed that BZT ceramics were crystallized into a single-phase perovskite structure. At room temperature, the splitting of (002) and (200) diffraction peaks of undoped BaTiO_3 ceramics confirms the tetragonal phase (see Fig. 1a). The corresponding diffraction angles are 44.9° and 45.3° , respectively. The two diffraction peaks gradually merge into one peak, confirming that the structure of the BZT system is undergoing a transformation from tetragonal to orthorhombic at room temperature. Therefore, it is concluded that the Zr doping in BaTiO_3 system can influence the structure and lattice parameter in order to maintain the perovskite structure. Similarly, the Zr doping in BaTiO_3 ceramics can also influence the dielectric properties (see Fig. 2). In the present study, 2θ is shifted slightly to a lower angle with increasing Zr composition, which indicates that the lattice parameter of the BZT12 ceramics is larger than that of BZT2. As the ionic radius of Zr^{4+} (0.98 \AA) is larger than that of Ti^{4+} (0.72 \AA), the lattice parameter of the BZT ceramics is expected to increase with increasing Zr composition: the Zr^{4+}

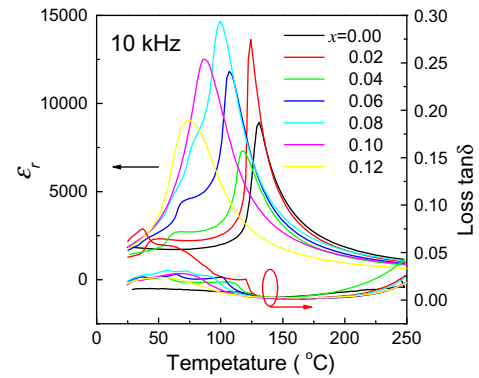


Figure 2. The dielectric permittivity and loss tangent as a function of temperature for $\text{Ba}(\text{Zr}_x\text{Ti}_{1-x})\text{O}_3$ samples at 10 kHz.

(0.98 \AA) ions of larger ionic radius occupy the B sites, replacing the Ti^{4+} (0.72 \AA). This indicates that the Zr^{4+} ions have entered the unit cell, and early X-ray crystalline structure studies also revealed that $\text{Ba}(\text{Zr}_x\text{Ti}_{1-x})\text{O}_3$ could form a complete solid solution [12].

Figure 2 shows the dielectric permittivity ϵ_r and loss $\tan \delta$ dependence of temperature for all of the $\text{Ba}(\text{Zr}_x\text{Ti}_{1-x})\text{O}_3$ samples with x from 0.02 to 0.12 at 10 kHz. For the BaTiO_3 sample, the phase transition temperature of cubic paraelectric to tetragonal ferroelectric (T_c) is observed at 131°C . For the ceramics with $x = 0.02$, the T_c is 124°C . In addition, T_c decreased nonlinearly from 124 to 74°C with increasing x (Zr content) from 0.02 to 0.12, respectively. There are some interesting characteristics in the BZT system. For the composition of $0.02 \leq x \leq 0.08$, on each curve of dielectric permittivity vs. temperature, another dielectric peak apart from the T_c peak is clearly noticeable. The temperature of this dielectric peak corresponds to the transition temperature from tetragonal to orthorhombic structure (T_{o-t}), which is a ferroelectric to ferroelectric phase transition. The T_{o-t} temperature can be obtained more clearly from the dielectric loss peak than from the dielectric permittivity.

Figure 3 shows phase transition temperature T_c and T_{o-t} , and maximum dielectric permittivity ϵ_m as functions of Zr-doping content x at 10 kHz for $\text{Ba}(\text{Zr}_x\text{Ti}_{1-x})\text{O}_3$ ceramics.

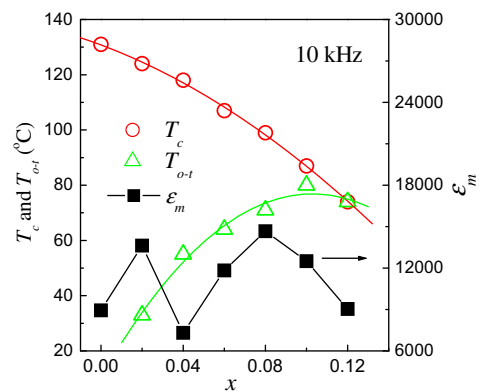


Figure 3. Phase transition temperature T_c and T_{o-t} , and maximum dielectric permittivity ϵ_m as functions of Zr-doping content x at 10 kHz for $\text{Ba}(\text{Zr}_x\text{Ti}_{1-x})\text{O}_3$ ceramics.

($\text{Zr}_x\text{Ti}_{1-x}\text{O}_3$) ceramics, and the T_{o-t} values from the dielectric loss peaks. It is found that the T_{o-t} increased nonlinearly from 33 to 80 °C with increasing x from 0.02 to 0.10, respectively. Furthermore, the T_{o-t} peak decreases with increasing x . When x equals 0.08, the T_c and T_{o-t} are 99 and 71 °C, respectively. As compared with previous results, the values of the phase transition temperatures are almost the same as those reported in the literature [11]. This is due to the curve of dielectric permittivity ε_r vs. temperature showing diffusivity. In this composition range, the BZT system is ferroelectric with a decreased paraelectric to ferroelectric phase transition temperature (i.e. T_c decreased) and increased ferroelectric to ferroelectric transition temperature (T_{o-t}); this is the so-called pinched phase transition [13]. For the pure BT ceramic, the ferroelectric phase transition temperature is lower than the Zr-doped ceramics, so the second dielectric peak cannot be observed in the temperature range measured here. However, for the composition BZT12, the two-phase transition is pinched into one dielectric peak due to the increased Zr content. In this case, the BZT12 ceramic has orthorhombic structure at room temperature. This agrees well with the XRD results.

From Figures 2 and 3, it could be observed that the temperature T_m corresponding to the maximum value of the dielectric permittivity ε_m decreases with increasing Zr content. Similarly, the BZT ceramics gradually show a broad dielectric permittivity–temperature curve in the vicinity of transition temperature, which is induced by an inhomogeneous distribution of Zr ions in the Ti sites and mechanical stress in the grain [9]. Generally, the substitution of Zr^{4+} ion in BaTiO_3 ceramics leads to a decrease in the Curie temperature. There are two reasons for this phenomenon. On the one hand, because the radius of the Zr^{4+} ion (0.98 Å) is larger than that of the Ti^{4+} ion (0.72 Å), substitution of Zr^{4+} for Ti^{4+} will weaken the bonding force between the B-site ion and the oxygen ion of the ABO_3 perovskite structure. As the B–O bonds are weakened, the B-site ion can resume its position only when the tetragonal ferroelectric is at lower temperature, so the phase transition temperature is reduced. On the other hand, the weakening of B–O bonds leads to a weaker distortion of the octahedron, and the replacement also might induce a “break” of the cooperative vibration of B–O chains; those could bring about a decrease in the c/a ratio. This “break” is responsible for the T_c of BZT system, thus a drop in Curie temperature was observed [10,14,15].

To describe the diffusivity of a phase transition, a modified Curie–Weiss law has been proposed [16]:

$$\frac{1}{\varepsilon_r} - \frac{1}{\varepsilon_m} = \frac{(T - T_m)^\gamma}{C'} \quad (1)$$

where γ and C' are assumed to be constant and $1 \leq \gamma \leq 2$. The parameter γ gives information on the character of the phase transition: for $\gamma = 1$, a normal Curie–Weiss law is obtained; $\gamma = 2$ describes a complete diffuse phase transition.

Figure 4 shows the plot of $\ln(1/\varepsilon_r - 1/\varepsilon_m)$ as a function of $\ln(T - T_m)$ for BZT4 sample at 10 kHz, and the inset shows the diffusivity factor as a function of Zr content. A linear relationship is observed for the seven samples. The slope of the fitting curves (using

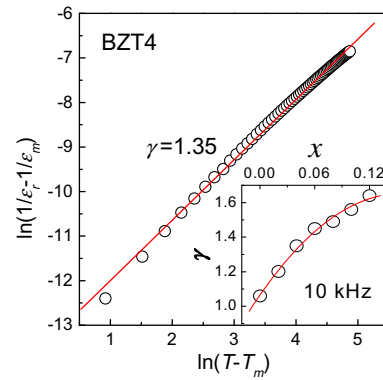


Figure 4. $\ln(1/\varepsilon_r - 1/\varepsilon_m)$ vs. $\ln(T - T_m)$ for BZT4 ceramic at 10 kHz, the inset shows the diffusivity factor as a function of Zr-doping contents.

Eq. (1)) is used to determine the γ value. The γ value of BZT4 ceramic is 1.35. The solid line is obtained by polynomial fitting. Like T_c vs. x , γ vs. x also exhibits a nonlinear relationship. The values of γ for BZT ceramics increase with increasing Zr content. For BT and BZT12, they are 1.06 and 1.64, respectively. The values of γ larger than 1 for all the BZT compositions show the gradual departure from the normal Curie–Weiss and the composition-induced diffuse transition.

There are many reasons for the relaxor behavior, such as a microscopic composition fluctuation, the merging of micropolar regions into macropolar regions, or a coupling of order parameter and local disorder mode through the local strain [10,17]. Vugmeister and Glinichuk reported that the randomly distributed electrical field/or strain field in a mixed-oxide system was the main reason leading to the relaxor behavior [17]. In perovskite-type compounds, the relaxor behavior appears when at least two cations occupy the same crystallographic site A or B. At the solid solution of $\text{Ba}(\text{Zr}_x\text{Ti}_{1-x})\text{O}_3$, the Zr and Ti ions co-occupy the B sites. The different effects of B-site substitution on cation ordering and the stability of the polar region are considered to be based on the polarizability of cations and the tolerance factor of the perovskite structure. For perovskites with the general formula of ABO_3 , the following equation can be used to calculate the tolerance factor, t [18]:

$$t = \frac{R_A + R_O}{\sqrt{2}(R_B + R_O)}, \quad (2)$$

where R_A is the radius of A-site atom, R_B is the radius of B-site atom and R_O is the radius of O atom.

As t increases, the normal ferroelectric phase becomes stabilized. Hence Ti^{4+} cations can stabilize the normal ferroelectrics phase in BT, while Zr^{4+} cations in B-sites behave as a typical destabilizer against normal ferroelectrics and induce paraelectric behavior due to their higher ionic diameter and lower polarization. In this case, more macrodomains (long-range ordered regions) in Zr-substituted ceramics will break up into micropolar regions than in pure BT ceramics. Thus, the BZT ceramics transform from the normal ferroelectrics to the relaxor ferroelectric due to the larger ionic diameter of Zr ions.

The effects of Zr doping on the phase transition and dielectric properties of a series of $\text{BaZr}_x\text{Ti}_{1-x}\text{O}_3$ ($0 \leq x \leq 0.12$) samples have been studied. The diffraction peaks shift to the lower angle with increasing of Zr-doping contents, accompanied by the phase transition from tetragonal to orthorhombic. We also find that the Curie temperature of pure BT is 131 °C, while BZT12 drops to 74 °C with almost a decrease nonlinearly. But the diffusivity factor γ increase from 1.06 to 1.64 for BT to BZT12 ceramics at a frequency of 10 kHz, implying a composition-induced diffuse transition. For the composition of $0.02 \leq x \leq 0.08$, the BZT ceramics exhibit a pinched phase transition of ferroelectric to ferroelectric phase transition; above this composition range, two of the phase transitions have merged into one dielectric peak.

This work is supported by the National Natural Science Foundation of China (Grant No. 10774030), the Science and Technology Program of Guangdong Province of China (Grant No. 2006A11003005), and the Science and Technology Program of Guangzhou City of China (Grant No. 2006Z3-D0211).

[1] J.F. Scott, C.A.P. de Araujo, *Science* 246 (1989) 1400.

[2] W. Zhang, X.G. Tang, K.H. Wong, H.L.W. Chan, *Scripta Mater.* 54 (2006) 197.

[3] Z.G. Xia, Q. Li, *Scripta Mater.* 57 (2007) 981.

[4] E. Dul'kin, E. Mojaev, M. Roth, Wook Jo, T. Granzow, *Scripta Mater.* 60 (2009) 251.

[5] X.G. Tang, H.Y. Tian, J. Wang, K.H. Wong, H.L.W. Chan, *Appl. Phys. Lett.* 89 (2006) 142911.

[6] Y.L. Wang, L.T. Li, J.Q. Qi, Z.L. Gui, *Ceram. Int.* 28 (2002) 657.

[7] W.Q. Cao, J.W. Xiong, J.P. Sun, *Mater. Chem. Phys.* 106 (2007) 338.

[8] X.G. Tang, J. Wang, X.X. Wang, H.L.W. Chan, *Solid State Commun.* 131 (2004) 163.

[9] X.G. Tang, K.H. Chew, H.L.W. Chan, *Acta Mater.* 52 (2004) 5177.

[10] S.G. Lee, D.S. Kang, *Mater. Lett.* 57 (2002) 1629.

[11] Z. Yu, R. Guo, A.S. Bhalla, *J. Appl. Phys.* 88 (2000) 410.

[12] C. Peng, J.F. Li, W. Gong, *Mater. Lett.* 59 (2005) 1576.

[13] Y. Zhi, A. Chen, R. Guo, A.S. Bhalla, *Mater. Lett.* 61 (2007) 326.

[14] W.R. Huo, Y.F. Qu, *Sens. Actuators A* 128 (2006) 265.

[15] N. Sawangwan, J. Barrel, K. Mackenzie, T. Tunkasiri, *Appl. Phys. A* 90 (2008) 723.

[16] K. Uchino, S. Nomura, *Ferroelectr. Lett. Sect.* 44 (1982) 55.

[17] B.E. Vugmeister, M.D. Glinichuk, *Rev. Mod. Phys.* 62 (1990) 993.

[18] S.K. Rout, E. Sinha, S. Panigrahi, *Mater. Chem. Phys.* 101 (2007) 428.